

Ground State Properties of the One-Dimensional Unconstrained Pseudo-Anyon Hubbard Model

Wanzhou Zhang,¹ Sebastian Greschner,^{2,*} Ernv Fan,¹ Tony C Scott,^{1,3} and Yunbo Zhang⁴

¹*College of Physics and Optoelectronics, Taiyuan University of Technology Shanxi 030024, China*

²*Institut für Theoretische Physik, Leibniz Universität Hannover, Appelstr. 2, DE-30167 Hannover, Germany*

³*Near India Pvt Ltd, no. 71/72, Jyoti Nivas College Road, Koramangala, Bengaluru 560095, India*

⁴*Institute of Theoretical Physics, Shanxi University, Taiyuan 030006, China*

(Dated: September 28, 2018)

We systematically study the (pseudo-) anyon Hubbard model (AHM) on a one-dimensional lattice without the presence of a three-body hardcore constraint. We analyze the effect of an induced hardcore constraint in the pseudo-fermion limit at statistical angles $\theta \rightarrow \pi$, which leads to the stabilization of superfluid ground state for vanishing or even small attractive on-site interactions. For finite statistical angles, we study the non-conventional broken-symmetry superfluid (BSF) peaked at a finite momentum, resulting in an interesting beat phenomenon of single particle correlation functions. In particular for $\theta \approx \pi$, we observe a wealth of exotic properties including a first order transition between different SF phases and a two-component partially paired phase (PP) for large fillings without the need of an additional three-body hardcore constraint. We show how the various superfluid ground state phases, including the PP phase, in the pseudo-fermion limit may be studied in an intuitive mean field frame.

I. INTRODUCTION

Bosons and fermions, are the two types of well-known elementary particles, respectively. By exchanging two bosons (fermions), the wave function is symmetric (anti-symmetric), or updated with a new phase factor $e^{i\theta}$, where $\theta = 0$ for bosons, and $\theta = \pi$ for fermions. In low dimensions, particles with other types of quantum statistics, anyons, are possible. Anyons are governed by statistics which are intermediate between those of bosons and fermions. The exchange of two identical anyons will acquire a phase angle θ , which can be of any value. Since the 1980s[1] anyons have attracted much physical interest and have become a very important concept in condensed matter physics including the fractional quantum Hall effect [2–6] and topological quantum computing [7, 8].

Experimentally, several schemes have been proposed to search for the anyons in spin or boson models[8–12] or in cold atoms[13–17]. During the last years ideas for the realization of (pseudo-) anyons in one dimensional optical lattices as initially proposed by Keilmann et al. [18] have attracted a large interest. Here, a Raman-assisted hopping scheme would allow for the manipulation and engineering of the anyonic exchange statistic at will in an optical lattice experiment. Recently, this experimental scheme for the realization of such anyon-Hubbard models (AHM) has been refined [19], drastically simplified [20] and extended to two-component anyons [21]. Typically these models are only valid in the low density regime or impose a three body hardcore-constraint, restricting the local particle number per site to $n_{max} = 2$. However, there have been proposals for the realization of AHM-like models [22] by means of modulated interactions without

this restriction.

While an experimental realization of one dimensional anyons on a lattice is still lacking, theoretically the physics of AHM has been studied extensively during the recent years. Properties of the hardcore AHM (i.e. with a constraint of local Hilbert space to 0 or 1 particles), the asymmetric momentum distributions [23, 24], intriguing particle dynamics [25, 26] and entanglement properties [27] have been studied.

Pseudo-AHMs [18] (or certain two-component AHMs [21, 28]), where the particles obey off-site anyon-like commutation relations and on-site, act like bosons, have been shown to exhibit a rich phase diagram dependent on the statistical angle θ . While previous studies of ground state properties focused on the analysis of modifications of the MI to SF transitions, including statistically induced Mott-insulator to superfluid quantum phase transitions [18, 29], properties of momentum distribution [30] and expansion dynamics [31], recently in Ref. [19] a wealth of further ground state phases of the AHM was described: dimerized phases and a novel two-component partially paired phase realized for statistical angles $\theta \rightarrow \pi$. Since the latter work focused on the AHM in the presence of an artificial three-body hardcore constraints due to the proposed experimental realization, it remained unclear whether or not the interesting ground state phases and in particular the PP phase can arise for the pseudo-AHM without further constraint on the local particle number.

In this work, we fill this gap and study the ground state phase diagram of the unconstrained AHM particularly focusing on statistical angles close to the pseudo-fermion limit $\theta \rightarrow \pi$. We discuss three fundamental properties of the AHM: effective statistically induced repulsive interactions, a density-dependent (drift of the) momentum distribution and the emergence of the exotic two-component PP phase.

*sebastian.greschner@itp.uni-hannover.de

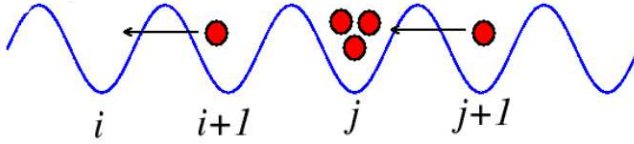


FIG. 1: The illustration of the conditional effect of $e^{i\theta n_i}$, $n_i = 0$, $e^{i\theta n_i} = 1$; $n_j = 3$, $e^{i\theta n_j} \neq 1$.

The paper is structured as follows: After an introduction to the model and methods (section II), we show the emergence of an effective Pauli exclusion principle induced by the anyonic exchange statistics which leads to a stabilization of particle density for vanishing interactions (see section III). In section IV, we analyze the asymmetric momentum distribution by means of mean field (MF) analysis and density matrix renormalization group (DMRG) simulations [32]. We study the crossover and transitions between superfluid phases condensed at a momentum $0 < \theta < \pi$ with broken reflectional symmetry (SF_Q or broken symmetry superfluid, BSF) and analyze the single particle correlation function. For $\theta = \pi$, we observe direct phase transitions between the SF₀ and SF _{π} phases. In section V, we present strong indications of an emergent two component phase PP phase at large fillings $\rho \gtrsim 1.5$. This phase can be understood as the presence of both an atomic and a paired superfluid component as we show by means of an intuitive mean-field and dilute limit picture for the PP phase. Concluding comments are made in Sec. VI.

II. THE MODEL, METHODS AND OBSERVABLES

A. Model

The starting point is the AHM,

$$H^\alpha = -t \sum_{i=1}^L (\alpha_i^\dagger \alpha_{i+1} + h.c.) + \sum_i h_i \quad (1)$$

where $\alpha_i^\dagger (\alpha_i)$ is the anyon creation (annihilation) operator at site i , t is the single-anyon hopping amplitude, L is the lattice size, and $n_i = \alpha_i^\dagger \alpha_i$ is the number operator of the anyons on site i . α_j and α_j^\dagger satisfy anyonic commutation relations, $\alpha_j \alpha_k^\dagger - e^{-i\theta \text{sgn}(j-k)} \alpha_k^\dagger \alpha_j = \delta_{jk}$ and $\alpha_j \alpha_k - e^{-i\theta \text{sgn}(j-k)} \alpha_k \alpha_j = 0$. In the term $h_i = \frac{U}{2} n_i(n_i - 1) - \mu n_i$, U is the on-site two-body interaction and μ is the chemical potential term. By a Jordan-Wigner transformation [18],

$$\alpha_j = b_j e^{-i\theta \sum_{i=1}^{j-1} n_i}, \quad (2)$$

where b_i is a boson annihilation operator, the anyon Hamiltonian H^α can be re-expressed as a Bose-Hubbard

model with a density dependent phase factor[18]:

$$H^b = -t \sum_{i=1}^L (b_i^\dagger b_{i+1} e^{i\theta n_i} + h.c.) + \sum_i h_i. \quad (3)$$

Fig. 1 shows the conditional effects of the density-dependent phase factor caused by $b_i^\dagger b_{i+1} e^{i\theta n_i}$. If there are no particles in the site i , namely $n_i = 0$, then the phase factor is still given by $e^{i\theta n_i} = 1$.

The situation becomes different for a soft-core Bose-Hubbard model, allowing of more than one particle on each site $n_{max} > 1$. If three particles already exist in the site j as shown in the example in Fig. 1, the phase factor becomes $e^{i\theta n_j} = e^{i3\theta}$.

B. The mean-field scheme

Apart from numerically exact DMRG calculations, which are performed with open and periodic boundary conditions keeping up to $m = 600$ states, we analyze the system by means of a (Gutzwiller)-mean-field scheme. Following Keilmann et al. [18], the density dependent hopping $b_j^\dagger e^{i\theta n_j} b_{j+1} = c_j^\dagger b_{j+1}$ is decoupled as

$$c_j^\dagger b_{j+1} \approx -\Psi_{2,j}^* \Psi_{1,j+1} + \Psi_{2,j}^* b_{j+1} + c_j^\dagger \Psi_{1,j+1},$$

where the order parameters are introduced as $\Psi_{1,j} = \langle b_j \rangle$ and $\Psi_{2,j} = \langle c_j \rangle$.

Assuming a homogeneous solution $\Psi_1 = \langle b_j \rangle = \langle b_{j+1} \rangle$, $\Psi_2 = \langle c_j \rangle = \langle c_{j+1} \rangle$, the decoupled Hamiltonian may be written as

$$H = -zt(\Psi_2 b^\dagger + \Psi_2^* b + \Psi_1 c^\dagger + \Psi_1^* c - \Psi_1^* \Psi_2 - \Psi_2^* \Psi_1) + \frac{U}{2} n(n-1) - \mu n. \quad (4)$$

where the coordination number $z = 2$. This system has to be solved self-consistently for Ψ_1 , Ψ_2 . The solution minimizes the energy functional $E(\Psi_1, \Psi_2)$, where $E(\Psi_1, \Psi_2)$ is the lowest eigenenergy of H for a given set of order parameters Ψ_1 and Ψ_2 [33].

One may easily extend the mean-field ansatz to larger unit cells. E.g. for a two site $L = 2$ unit cell, we use subscripts A and B to distinguish the physical quantities Ψ_1 and Ψ_2 , on the different sublattices, such as Ψ_{1A} , Ψ_{1B} , Ψ_{2A} , and Ψ_{2B} . We define the average density of atoms on both sublattices as $\rho_A = \langle n_A \rangle$ and $\rho_B = \langle n_B \rangle$. Combining Eq. (4) and the definitions of order parameters, we obtain the local Hamiltonian on the sublattice A and thus

$$H_A = -\frac{zt}{2} [c_A^\dagger \Psi_{1B} + c_A \Psi_{1B}^* + b_A \Psi_{2B}^* + b_A^\dagger \Psi_{2B}] - \frac{1}{2} (\Psi_{2A}^* \Psi_{1B} + \Psi_{2A} \Psi_{1B}^* + \Psi_{2B}^* \Psi_{1A} + \Psi_{2B} \Psi_{1A}^*) + \frac{U}{2} n_A(n_A - 1) - \mu n_A, \quad (5)$$

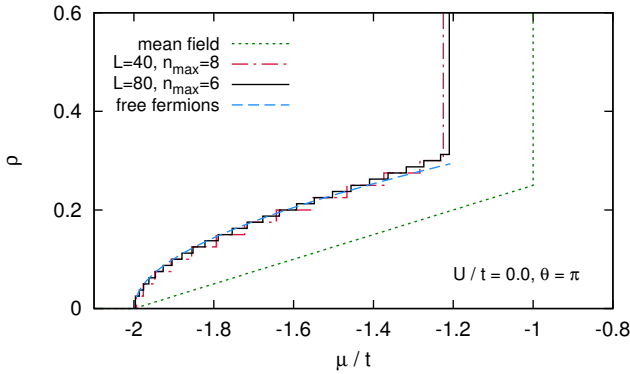


FIG. 2: Equation of state $\rho = \rho(\mu)$ for the AHM for a statistical angle $\theta = \pi$ and vanishing on-site interactions $U = 0$. Both DMRG and MF methods show a stabilization of a SF phase for small fillings and a collapse after some critical filling factor. The MF-case overestimated this point to $\mu/t = -1$, while the true value is around $\mu/t \approx -1.2$ as seen by the DMRG calculation.

and the Hamiltonian on H_B is

$$H_B = -\frac{zt}{2} [b_B^\dagger \Psi_{2A} + b_B \Psi_{2A}^* + c_B^\dagger \Psi_{1A} + c_B \Psi_{1A}^* - \frac{1}{2} (\Psi_{2A}^* \Psi_{1B} + \Psi_{2A} \Psi_{1B}^* + \Psi_{2B}^* \Psi_{1A} + \Psi_{2B} \Psi_{1A}^*)] + \frac{U}{2} n_B (n_B - 1) - \mu n_B \quad (6)$$

Again Eqs. (5) and (6) have to be solved self-consistently. Analogously we treat systems with larger unit cells up to $L = 10$.

III. EFFECTIVE REPULSIVE INTERACTIONS AND STABILIZATION FOR VANISHING INTERACTIONS

The density dependent Peierls phase induces an effective repulsion which has important consequences on the ground state phase diagram. A variation of the statistical angle θ may induce SF to MI transitions as observed in Refs. [18, 29]. In Refs. [19, 22] this property has been explained from the point of view of a weak coupling analysis, in which the Luttinger liquid (LL) parameter is $K = \pi/(\theta^2 + \frac{U}{2\rho J})^{1/2}$. Hence the statistical angle θ has qualitatively the same effect as a repulsive $U > 0$.

We can explore this effect further in the MF-frame for the pseudo-fermion limit. In this regime, a self-consistent ground state solution with $\Psi_1 = \Psi_2 \equiv \Psi$ can be found. Then, due to the assumption of a density dependent correlated hopping $b^\dagger (-1)^n b$, the Hamiltonian reduces to a block-diagonal form with the hopping term only coupling Fock-states $|0\rangle$ and $|1\rangle$, $|2\rangle$ and $|3\rangle$, etc. For the low density case, the Hamiltonian in the sector of 0 and

1 particles is given by

$$H_{0,1} = 2t \begin{pmatrix} |\Psi|^2 & -\Psi \\ -\Psi^* & |\Psi|^2 - \mu/2t \end{pmatrix} \quad (7)$$

For $\mu/J > -2$, one easily obtains a solution with $\Psi \rightarrow \sqrt{4J^2 - \mu^2}/(4J)$ and the density is given by $\langle n \rangle = (2 + \mu/J)/4$ as shown in Fig. 2. For $\mu > -J$, the system becomes unstable and it is energetically favorable to form a macroscopically occupied site seen by the (infinitely) large jump in density in the $\mu - \rho$ -curve. One may easily generalize this solution for finite U/t and sub-sectors of n and $n + 1$ particles

$$H_{n,n+1} = \begin{pmatrix} 2|\Psi|^2 t - \mu n + \frac{(n-1)nU}{2} & -2\Psi t \sqrt{1+n} \\ -2\Psi^* t \sqrt{1+n} & 2|\Psi|^2 t - \mu(1+n) + \frac{n(1+n)U}{2} \end{pmatrix} \quad (8)$$

which gives rise to the solution

$$\Psi_{n,n+1} \rightarrow \frac{\sqrt{4t^2 - \mu^2 + 8t^2n + 4t^2n^2 + 2\mu n U - n^2 U^2}}{4t\sqrt{1+n}} \quad (9)$$

An example for this case will be shown below in section V. Interestingly, the $\Psi_{0,1}$ solution remains stable also for small attractive interactions $U/J < 0$.

So, remarkably, the fermionic off-site exchange statistics already induces a Pauli exclusion principle, i.e. a hardcore constraint for low fillings. We verify this property by means of DMRG calculations as shown in Fig. 2. The low density part of the $\mu - \rho$ -curve has an almost perfect overlap with the corresponding result from free (hardcore) fermions, for which $\rho = \arccos(-\mu/2t)/\pi$. The DMRG-calculation indicates a slightly lower bound $\mu/t \approx -1.2$ for the instability of the system.

IV. SF₀, SF_π AND BROKEN SYMMETRY SUPERFLUID PHASES

A. Asymmetric momentum distribution

A very important property of one dimensional anyons discussed in Ref.[18] is the asymmetric momentum distribution of the original bosonic particles, due to the broken space-reversal symmetry resulting from the phase factor assigned to the hopping. As shown by Refs[23, 24, 30], the total bosonic momentum distribution

$$n(k) = \frac{1}{L} \sum_{i,j} \langle b_i^\dagger b_j \rangle e^{ik(i-j)}. \quad (10)$$

emerges in single peaks at some momentum Q which are asymmetric with $k = 0$.

One may easily understand the asymmetry of the momentum distribution from the assumption of a system

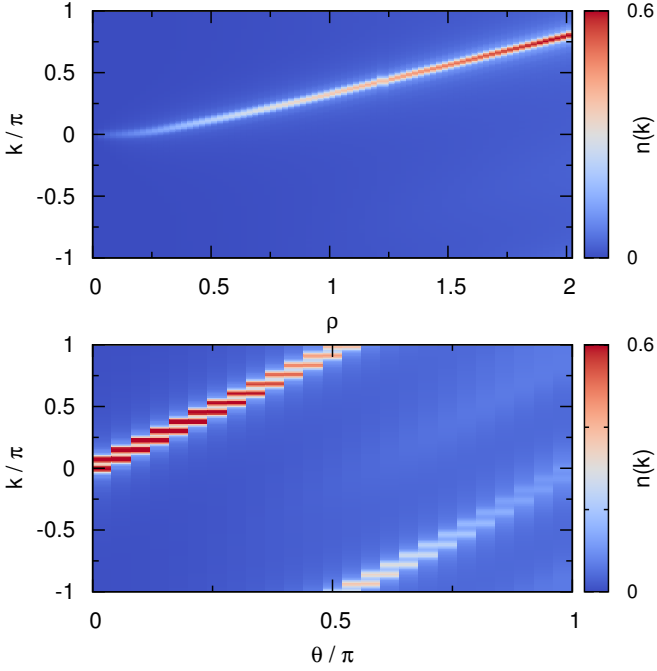


FIG. 3: (a) (Bosonic) momentum distribution $n(k)$ for the AHM ($L = 40$, $n_{max} = 4$) as a function of the density for a statistical angle $\theta = \pi/2$. The system is always in a superfluid state. Apparently we do not observe any phase transitions. (b) (Bosonic) momentum distribution $n(k)$ for the AHM ($L = 40$, $n_{max} = 4$) as a function of the statistical angle θ/π for a density $\rho = 93/40$. The system is always in a superfluid state.

with a fixed density, $n_i \rightarrow \rho$. Taking this into account, the hopping-part of Hamiltonian (3) is given by

$$\begin{aligned} & \sum_i (b_i^\dagger b_{i+1} e^{i\theta\rho} + b_i^\dagger b_{i-1} e^{-i\theta\rho}) \\ &= \sum_k b_k^\dagger b_k (e^{ik+i\rho\theta} + e^{-ik-i\rho\theta}) \end{aligned} \quad (11)$$

Therefore, $E(k) = -2t \cos(k + \theta\rho)$ and should be asymmetric with $k = 0$ if $\theta\rho \neq 0$. One denotes this superfluid phase quasi condensing in $0 < Q < \pi$ due to the (externally) broken reflectional symmetry a broken symmetry superfluid (BSF) phase or generally SF_Q .

In Figs. 3 (a) and (b), we present the momentum distribution of Model (3) as a function of θ for $\rho \approx 2.3$ and as a function of the density ρ for $\theta = \pi/2$ which illustrates its strong dependence on filling and statistical angle. In general, SF_0 , BSF and SF_π phases are smoothly connected, and the peak-position of the momentum distribution Q continuously depends on density or statistical angle.

B. Staggered distribution of the SF_0 and SF_π phases

In this section, we study the distribution of superfluid phases within the mean field approach. Mainly we find

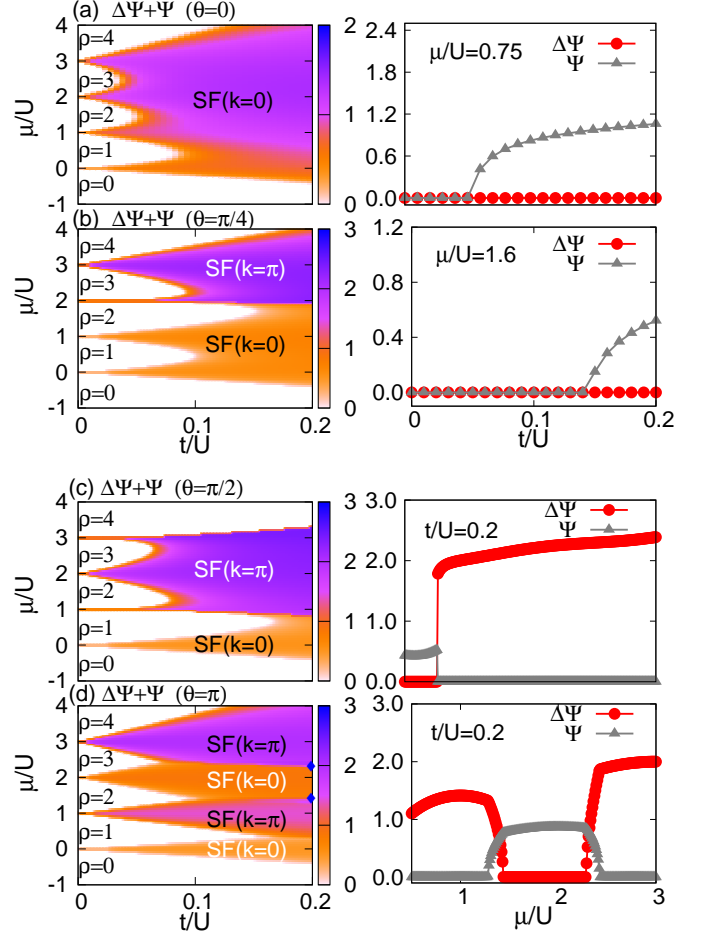


FIG. 4: (Color online) The quantum phase ($\Psi + \Delta\Psi$), which contains the SF_0 , SF_π and MI phases in the plane $(t/U, \mu/U)$ of the model with (a) $\theta = 0$, (b) $\pi/4$, (c) $\pi/2$, and (d) π , on the left column, from top to bottom sequentially. The right column are detailed descriptions of Ψ and $\Delta\Psi$ along t/U or μ/U .

a MF-solution with $|\Psi_1|^2 = |\Psi_2|^2$, the phase between Ψ_1 and Ψ_2 is fixed to a particular value $\arg(\Psi_2^* \Psi_1) \sim \theta \cdot \rho$ and $||\Psi_1|^2 - |\Psi_2|^2| = 0$. For a larger unit cell $L = 2$, the relative phase between different sites is found to be $\arg(\Psi_{1A}^* \Psi_{1B}) = 0$ or π , corresponding to the SF_0 and SF_π phases.

For the two-site unit cell, we introduce the average quantities $\rho = (\rho_A + \rho_B)/2$ and the SF density is $\Psi = |\Psi_{1A} + \Psi_{1B}|/2$. SF_0 phase and the SF_π phase may be distinguished by $\Delta\Psi = |\Psi_{1A} - \Psi_{1B}|$, which obviously vanishes for SF_0 , while $\Delta\Psi \neq 0$ for SF_π .

In Fig. 4, we present the global phase diagrams close to the MI regime, by plotting $\Psi + \Delta\Psi$ in the plane $(t/U, \mu/U)$ for θ at $0, \pi/4, \pi/2$ and π . As stated above, the results are obtained in a $L = 2$ unit cell system but we verify by comparison to larger L systems, which are commensurate with θ , that these results are correct. For this simple MF-scheme the relative phases in the ground state configuration are always pinned to 0 or π (even for the

presence of a phase $\theta \neq 0, \pi$) and hence a two-site unit cell offers complete insight into the mean-field properties.

At small t/U , with the maximum on-site occupation being $n_{max} = 4$, the MI phases emerge sequentially with densities $\rho = 0, 1, 2, 3$ and 4 when the chemical potential μ/U increases from 0 to 4. As discussed by Ref. [18], the MI phases are strongly enhanced by increasing ϕ due to the effective repulsion discussed in the previous section III. At larger t/U , a transition to the superfluid SF₀ and SF _{π} phases is observed.

In Fig. 4(a), for $\theta = 0$, the SF₀ phase emerges with finite values of t/U . As shown in the right column at $\mu/U = 0.75$, in the range $t/U > 0.05$, the SF₀ phase is localized with $\Psi \neq 0$ and $\Delta\Psi = 0$. By increasing t/U , Ψ changes continuously into a non-zero regime, which means the MI-SF₀ phase transition is continuous.

For $\theta > 0$, we observe a staggered pattern of SF _{π} and SF₀ phases. For $\theta \gtrsim \pi/2$ in the range of parameters of Fig. 4, we find the possibility of a direct phase transition from the SF₀ to SF _{π} phases. Ψ and $\Delta\Psi$ exhibit a sharp jump indicating a first order transition between the phases, as exhibited for cuts of the order parameters as shown in the right panel of Fig. 4 (c).

In Fig. 4(d), for $\theta = \pi$, more of the SF₀ and SF _{π} phases emerge from top to bottom. Interestingly, as can be seen from the left panel of Fig. 4 (d) the phase transition between the SF₀ and SF _{π} phases becomes continuous and we observe an intermediate phase with both superfluid order parameters Ψ and $\Delta\Psi$ being finite; these are labeled by two blue diamond symbols in the left Fig. 4(d). We will discuss this in detail in the following section V.

The mean-field analysis obviously fails for $0 < \theta < \pi$, not being able to describe the BSF-phase or the show the smooth transition between BSF phases observed from the DMRG data. However, the situation is different, not only for $\theta = 0$ but also for the pseudo-fermion limit $\theta = \pi$. As discussed in section V, DMRG-simulations show that for $\theta \approx \pi$ we indeed observe a staggered pattern of SF₀ and SF _{π} phases (and direct phase transitions or additional intermediate phases).

C. Single particle correlation

In the following, we discuss properties of the single particle correlation function $C(r) = \langle b_i^\dagger b_{i+r} \rangle$ which exhibits an interesting beat phenomenon related to the asymmetry of the momentum distribution characteristic for the non-conventional BSF phase. For a SF _{Q} superfluid-phase at a quasi-condensing at Q , with a momentum distribution peaked at Q additional to the algebraic decay typical for one-dimensional Luttinger liquids (see Fig. 5) we observe oscillatory pattern. For $\pi/2 < Q \bmod \pi < \pi$ both real and imaginary part of the correlation function may exhibit a beat pattern as shown in Fig. 5 (c) and (d) as $\text{Re}C(r) \sim \cos(Qr)$ and $\text{Im}C(r) \sim \sin(Qr)$.

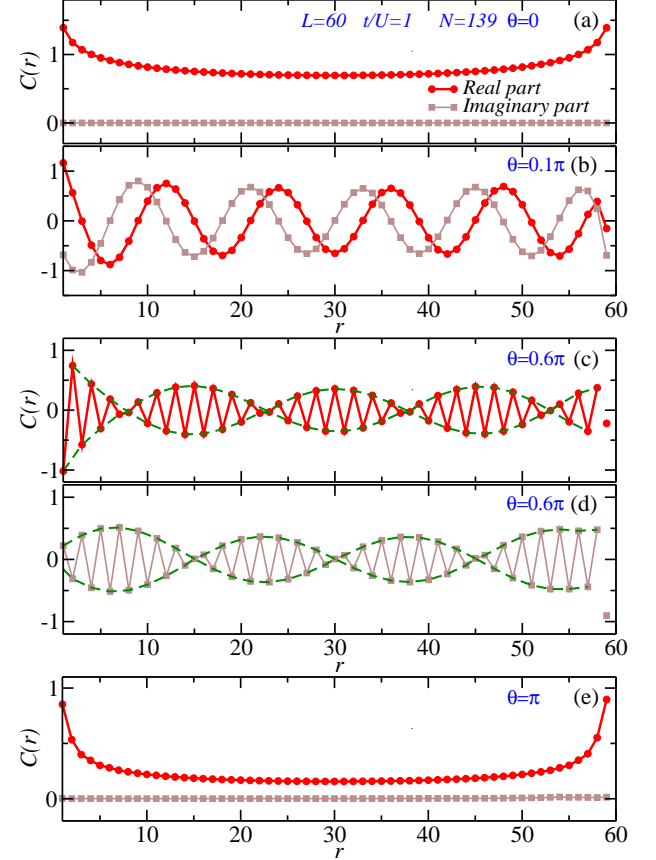


FIG. 5: (Color online) Emergence and disappearance of beats from both of the real and imaginary parts of the correlation $C(r)$ by modulation of θ for $\theta/\pi = 0, 0.1, 0.6$ and 1 at $t/U = 1$, $\rho = 139/60$.

V. THE PP PHASE FOR PSEUDO-FERMIONS

For the constrained AHM, the PP phase was first described in Ref. [19] and studied extensively using DMRG simulations. It may extended to quasi-1D ladder models [34] and also a variant of hardcore two-component AHM may exhibit a similar multicomponent PP phase [21].

A. The PP phase in the MF frame

As already observed in Fig. 4 for $\theta \sim \pi$, one observes a small intermediate region between the SF₀ and SF _{π} phases, the PP phase anticipating the following discussion. While within the mean field framework, the SF phases are characterized by $|\Psi_1| = |\Psi_2|$, for $\theta \rightarrow \pi$, interestingly, we find a second type of ground state solution, namely the relative phase and amplitude of Ψ_1 and Ψ_2 may fluctuate, while the total amplitude,

$$\chi_+^2 \equiv |\Psi_1|^2 + |\Psi_2|^2, \quad (12)$$

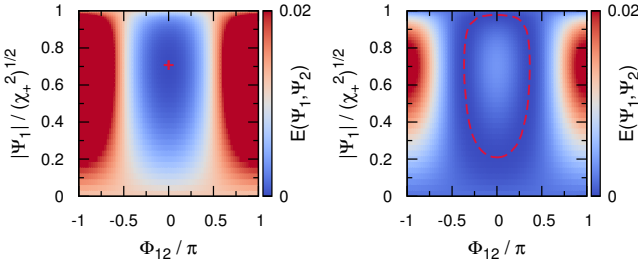


FIG. 6: (Color online) Energy functional $E(\Psi_1, \Psi_2)$ as a function of the relative phase Φ_{12} and amplitude $|\Psi_1|$ for (a) $\mu/U = 0.16$ (SF₀-phase) and (b) $\mu/U = 0.19$ (PP phase) for $t = 0.4U$ (for fixed $|\Psi_1|^2 + |\Psi_2|^2 \equiv \chi_+^2$). The red symbol and the dashed line mark the minima as obtained by a self-consistent solution of the mean-field equations.

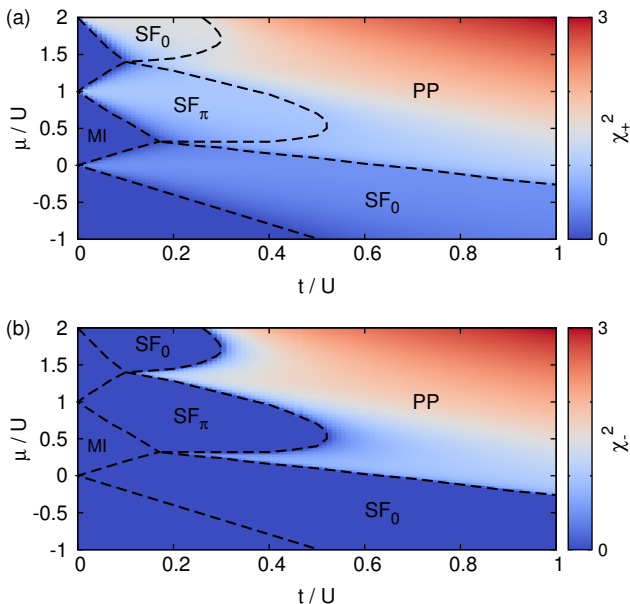


FIG. 7: (Color online) Mean field phase diagram for $t/U = 0.4$ as a function of t/U and μ/U ($n_{max} = 10$ bosons). Shadings indicate (a) the total superfluid density $|\Psi_1|^2 + |\Psi_2|^2$ and (b) the relative SF density $||\Psi_1|^2 - |\Psi_2|^2||$

is fixed. In Fig. 6, we illustrate the energy functional $E(\Psi_1, \Psi_2)$ Eq. (4) as a function of the amplitude $|\Psi_1|$ and the relative phase $\Phi_{12} = \arg(\Psi_1) - \arg(\Psi_2)$. Its minima correspond to the set of self-consistent solutions of the meanfield equations (4). For SF phase there is only one minimum (see Fig. 6 (a)) corresponding to the case $|\Psi_1| = |\Psi_2|$ with the spontaneously broken $U(1)$ symmetry of the overall phase and the superfluid order parameter χ_+^2 . However, for the PP phase, we find a solution spontaneously chosen from a one-dimensional manifold of degenerate minima as illustrated in Fig. 6 (b). In this phase of two-superfluid components, the PP phase, we

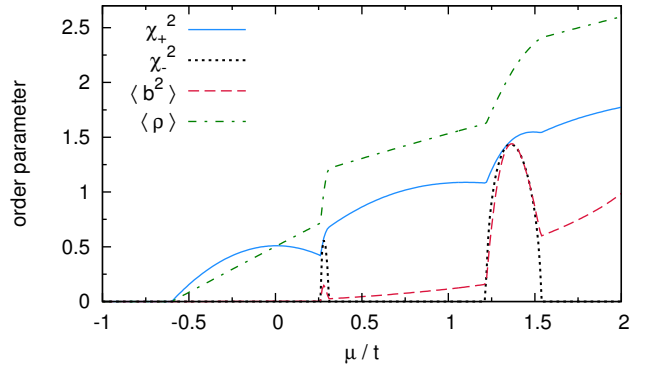


FIG. 8: Superfluid order parameters, average density and pair-density for $\theta = 0.9\pi$ and $t = 0.4U$ as a function of μ/U .

may define another order parameter

$$\chi^2_- \equiv \max | |\Psi_1|^2 - |\Psi_2|^2 |. \quad (13)$$

For the case shown in Fig. 6 the maximum is realized for a vanishing relative phase $\Phi_{12} \rightarrow 0$.

In Fig. 7, we show the full MF-phase diagram of pseudo-fermions. Interestingly, there are several lobes of effective hardcore superfluid phases SF_0 and SF_π separated by the intermediate PP phase which occupies a large part of the phase diagram for small U/t and large fillings $\rho \gtrsim 1$.

With the hardcore-solution Eq.(9), we find $\chi_+^2(n, n+1) = \frac{4J^2(1+n)^2 - (\mu - nU)^2}{8J^2(1+n)}$ and obviously χ_-^2 and also the pair-density $\langle b^2 \rangle$ vanish. However, the PP phase exhibits an enhanced pairing $\langle b^2 \rangle \sim \chi_-^2$. We may interpret the PP phase as a phase of both a (hardcore)-SF component and a partial formation of bound pairs on top of this background. Hence, this phase naturally extends the PP phase discussed for three-body constrained anyons in Ref. [19].

As depicted in Fig. 8 the PP phase may also be defined away from $\theta = \pi$ as seen by the order parameters $\chi_+^2 \neq 0$ and $\chi_-^2 \neq 0$. Here, for $\theta \neq \pi$ the pairing $\langle b^2 \rangle$ is also non-vanishing for the SF-phases, while $\chi_-^2 = 0$, which justifies the definition of the separate order parameter χ_+^2 .

It is important to note, that the equation of state $\rho = \rho(\mu)$ exhibits a kink at the SF-PP transition. The PP phase has a much larger compressibility, however finite.

B. Two-particle picture

As already shown in Refs. [19, 21] in the dilute limit $\rho \rightarrow 0$, we may derive an description of the properties of the AHM by means of a two-particle scattering problem [35]. A general two-particle state may be described by

$$|\Psi_K\rangle = \sum_x c_{x,x} (b_x^\dagger)^2 |0\rangle + \sum_{x,y>x} c_{x,y} b_x^\dagger b_y^\dagger |0\rangle. \quad (14)$$

We may express the amplitudes as $c_{x,x+r} = C_r e^{iQ(x+\frac{r}{2})}$ due to the conservation of total momentum $Q = k_1 + k_2$ in the scattering process. Taking this into account,

the Schrödinger equation $H |\Psi\rangle = \Omega |\Psi\rangle$ reduces to the following system of coupled equations:

$$(\epsilon_2 - U)C_0 = -\sqrt{2}t \left(e^{-i\frac{Q}{2}} + e^{i\left(\frac{Q}{2}+\theta\right)} \right) C_1 \quad (15)$$

$$\epsilon_2 C_1 = -\sqrt{2}t \left(e^{i\frac{Q}{2}} + e^{-i\left(\frac{Q}{2}+\theta\right)} \right) C_0 + 2t \cos\left(\frac{Q}{2}\right) C_2 \quad (16)$$

$$\epsilon_2 C_r = -2t \cos\left(\frac{Q}{2}\right) (C_{r-1} + C_{r+1}), \quad r \geq 2 \quad (17)$$

Let us first consider scattering states of two particles for which, in the thermodynamic limit, the energy is given by $\Omega = \epsilon(k_1) + \epsilon(k_2) = -4t \cos(q) \cos\left(\frac{Q}{2}\right)$ where $q = (k_1 - k_2)/2$. We may solve this set of equations with the ansatz $C_r = e^{-iqr} + e^{2i\delta} e^{iqr}$. The coefficients C_0 and δ are determined by Eqs. (15) and (16) and hence, are affected by the interactions and anyon statistics. From the scattering phase shift δ , we can extract the scattering length,

$$a = \frac{t(1 + \cos \theta)}{-2(2t + U) + 4t \cos \theta}. \quad (18)$$

By comparison to a 1D Bose gas of particles with mass m and contact interaction, one may identify a with an effective interaction strength $g = -2/(am)$ [35]. The scattering length diverges for $\theta \rightarrow 0, 2\pi$ but remains finite and negative for any other phase θ . This again shows the effective repulsion induced by the anyonic exchange statistics. For $\theta \rightarrow \pi$, the scattering length $a \rightarrow 0$ and, hence, the system approaches the Tonks limit $K \rightarrow 1$ of a hardcore free (fermion) gas as already discussed in section III.

An apparently counterintuitive observation is, that in spite of this effective hardcore character of the two particle scattering state, nonetheless a low-lying bound-states of two particles may exist (see also discussion in Ref. [21]). In order to analyze the two-particle bound states, we use the ansatz $C_r = \alpha^r$ with $|\alpha| < 1$ such that the solution is exponentially localized to its center of mass. We may again solve Eqs. (15)-(17) with this ansatz. Note, that for the usual Bose-Hubbard model $\theta = 0$ for repulsive interactions $U > 0$ a stable solutions of repulsively bound-pairs is found only for high energies above the two-particle scattering spectrum. The AHM for $\theta \rightarrow \pi$, however, for any U (repulsive or attractive) exhibits two different bound state solutions close to $Q \sim \pi$ as shown in Fig. 9, with energies given by

$$\epsilon_{\pm}^B = \frac{2U \cos(k) \pm (\cos(k) - 1) \sqrt{U^2 + 8t^2(1 - 3 \cos(k))}}{3 \cos(k) - 1} \quad (19)$$

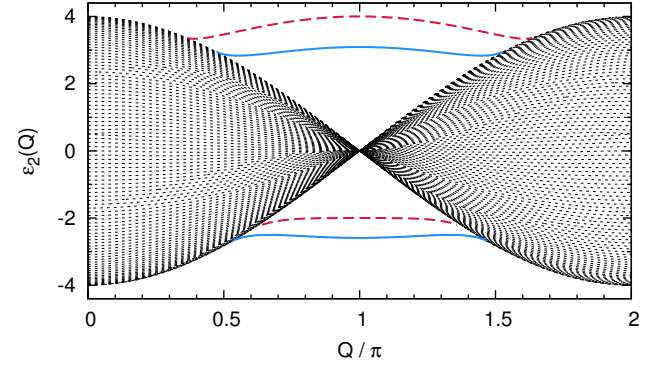


FIG. 9: (Color online) Emergence of bound-states in the two-particle spectrum $\epsilon_2(k)$ of the AHM for $\theta = \pi$. Dotted black lines illustrate the energies of two-particle scattering solutions. The solid (blue) and dashed (red) lines denote the stable bound state solutions for repulsive interactions $U = 0.5t$ and $U = 2t$ resp.

Interestingly, for any $U > 0$ one of these solutions has energies inside the two-particle spectrum $\epsilon_+^B < 0$. For $U < 2t$, it exhibits a local minimum at $Q = \pi$.

As discussed in Refs. [19, 21], we may now understand the exotic PP phase in a simplified picture as a phase of the simultaneous presence of both a gas of strongly repulsively interacting unpaired particles and a quasi-condensate of pairs (corresponding to the minimum of the low-lying bound state solution). Since, ϵ_+^B is not the lowest energy of the two-particle solution (as long as $U > -2t$), we may not expect a pure pair (quasi)-condensate such as the PSF phase studied for attractive interactions [36]. Neglecting interactions between these two quasi-particles, which may be reasonable for small densities of atoms ρ_a and pairs ρ_p , one may write a simplified model of the AHM as

$$H_{eff} = -2t \sum_k \cos(k) a_k^\dagger a_k + \sum_k \epsilon_-^B(k) b_k^\dagger b_k \quad (20)$$

where a_x (a_x^\dagger) and b_x (b_x^\dagger) are annihilation (creation) operators of hardcore atom and bound-pairs of momentum

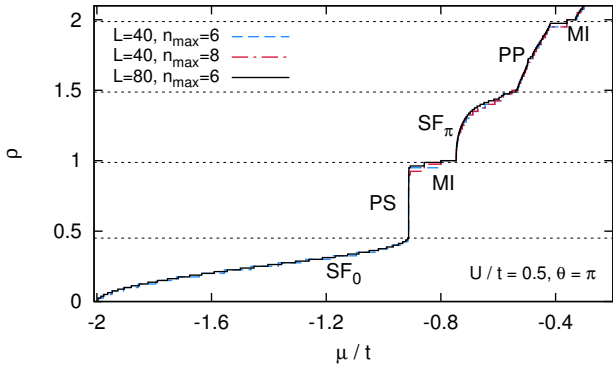


FIG. 10: (Color online) Equation of state $\rho = \rho(\mu)$ for the AHM for a statistical angle $\theta = \pi$. Several different phases and phase transitions may be observed. Interestingly there seems to be stable realization of PP-like phase.

k. The Hamiltonian has to be minimized under the constraint $\rho_a + 2\rho_p = \rho$. Although being certainly an oversimplification, Model (20) captures some main physical aspects: at low densities the ground state only contains species *a*; for higher fillings both species are present.

We may expand this dilute limit analysis to larger fillings by assuming the presence of a uniform and constant background filling *n*. Hence, the single particles moving on top of this background $|n+1\rangle$ and the bound-doublon-pairs $|n+2\rangle$ obtain a renormalized hopping rate due to the bosonic enhancement. By repeating the above analysis of bound and scattering states, we obtain a qualitatively similar picture for small $n = 1, 2, \dots$.

C. DMRG results

In order to overcome the limitations of the dilute limit picture, which does not take into account interactions between the effective particles, as well as the mean-field analysis (in one-dimension), we now examine the possibility of a PP phase by means of DMRG simulations of the unconstrained pseudo-AHM. We again make sure that our results are independent of the system size and the bosonic cut-off n_{max} .

In Fig. 10, we show the equation of state $\rho = \rho(\mu)$ for $\theta = \pi$ and small repulsive interactions $U = t/2$. Interestingly, the $\rho - \mu$ curve qualitatively compares well to the results of a mean-field calculation such as in Fig.8. We may identify several regimes. Also the effective hardcore phase SF_0 , as discussed above, is realized for $0 < \rho \lesssim 0.5$. While for larger densities $0.5 \lesssim \rho \lesssim 1$, the mean-field picture suggests a PP phase with a high compressibility, the DMRG-analysis shows that interactions between pairs and atoms lead to an instability of the system, characterized by a large macroscopic jump in density and a separation of phases (PS).

As discussed above for $\theta \rightarrow \pi$, we still observe MI phases at small interaction strengths, which can be iden-

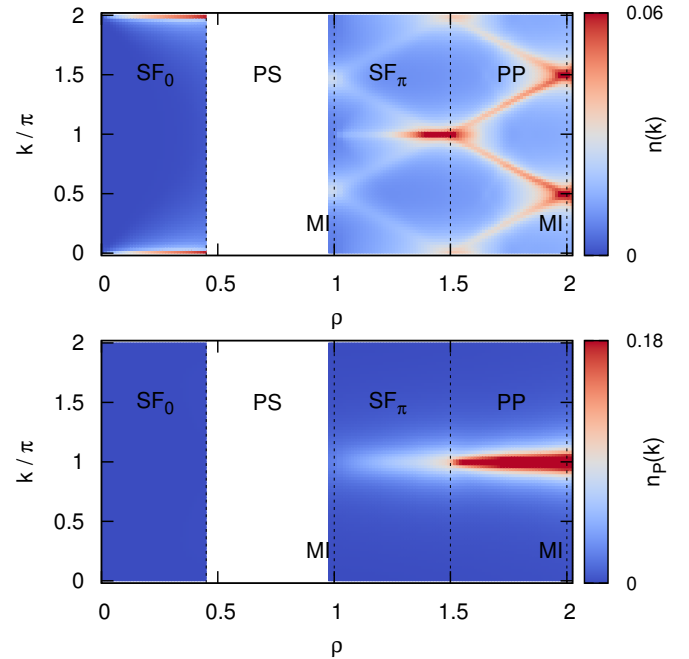


FIG. 11: (Color online) (Bosonic) momentum distribution $n(k)$ (a) and pair momentum distribution $n_P(k)$ (b) for the AHM ($L = 80$, $n_{max} = 6$) as a function of the density for a statistical angle $\theta = \pi$. We do not display data for the PS-region.

tified by the plateaus in the $\mu - \rho$ -curve at $\rho = 1$ and $\rho = 2$. Note that the step-like behavior of the plateaus is an effect of finite system size and open boundary conditions.

For large fillings, the mean field analysis predicts a PP phase with a much smaller compressibility. Indeed, for $\rho \sim 1.5$, we observe a pronounced kink in the $\mu - \rho$ of Fig. 10 curve which indicates a commensurate-incommensurate transition from the one-component SF_π to the two component PP phase as discussed in Ref.[19]. The scaling of the entanglement-entropy is consistent with a central-charge $c = 1$ in the SF- and $c = 2$ in the PP region (data not shown).

The most characteristic signature of the PP phase is given by its (bosonic) momentum-distribution function $n(k)$, which exhibits a characteristic multi-peak structure as shown in Figs. 11 (a) and 12. The largest peak is located at incommensurate values $k \neq 0, \pi$. Interestingly, also the SF_π phase exhibits several local maxima, in addition to the distinct peak at $k = \pi$. We also evaluate the pair-momentum distribution

$$n_p(k) = \sum_{i,j} e^{i(i-j)k} \langle \left(b_i^\dagger \right)^2 b_j^2 \rangle, \quad (21)$$

which is shown in Fig. 11 (b). As conjectured in the dilute limit analysis, we see the formation of a sharp peak at $k = \pi$, indicating a quasi-condensation of pairs in the PP phase.

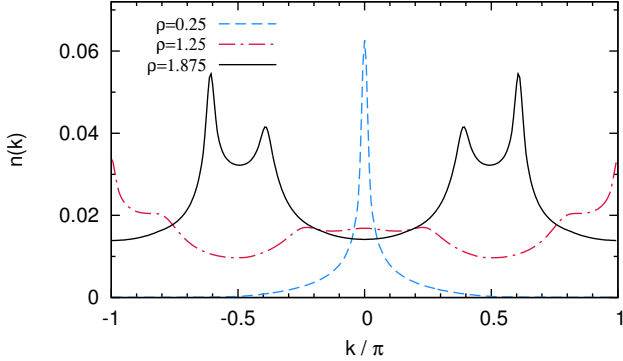


FIG. 12: (Color online) (Bosonic) momentum distribution $n(k)$ for the AHM ($L = 80$, $n_{max} = 6$, $U = 0.5t$) for a statistical angle $\theta = \pi$ and densities $\rho = 0.25$ (SF₀-phase), $\rho = 1.25$ (SF_π-phase) and $\rho = 1.875$ (PP phase).

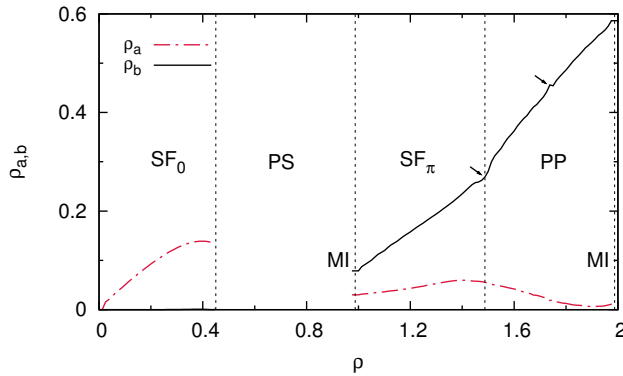


FIG. 13: (Color online) Sum of local single- ρ_a and two-particle correlations ρ_b ($L = 80$, $n_{max} = 6$, $U = 0.5t$) as defined in the main text. Arrows indicate interesting plateau-like substructure in the ρ_b -curve.

In Ref. [19], the atom and doublon-dimerizations,

$$\begin{aligned} \rho_a &= \frac{2}{L} \sum_{L/4 < i < 3L/4} \langle b_i^\dagger b_{i+1} \rangle, \\ \rho_b &= \frac{2}{L} \sum_{L/4 < i < 3L/4} \langle (b_i^\dagger)^2 (b_{i+1})^2 \rangle, \end{aligned} \quad (22)$$

have been shown to be a good probe for the PP and SF phases. In Fig. 13, we present ρ_a and ρ_b as a function of the density for the parameters of Fig. 10. This picture again proves that the low density SF₀ phase is a LL phase of almost hardcore single particles ($\rho_b \approx 0$). Contrary to the outcome of the mean-field analysis, this is not true for the SF_π phase for $1 \lesssim \rho \lesssim 1.5$. Here, we observe both finite $\rho_a, \rho_b > 0$ and a linear increase of both quantities with the density. However, the PP phase is characterized by a enhanced increase of ρ_b while ρ_a decreases.

Apparently, the $\rho_d - \rho$, but also the $\mu - \rho$ curve of Fig. 10, exhibit some kind of interesting substructure.

One may observe several small plateau-like steps at certain commensurate fillings $\rho \approx 1.5$ and $\rho \approx 1.75$ which could indicate the formation of pair-crystals due to an effective pair-pair interaction. Similar plateaus at fractional fillings have also been observed in Ref. [18] for a trapping potential. We will postpone a detailed study of this interesting phenomenon to a subsequent work.

VI. CONCLUSION

In summary, we have systematically studied the ground state physics of the pseudo-AHM on a one dimensional lattice without a constraint on local particle number. By using the DMRG and MF methods, we have analyzed its characteristic and exotic properties.

We have discussed how the anyonic exchange statistics may induce an effective repulsion. For the case of pseudo-fermions and a statistical angle $\theta = \pi$, the fermionic off-site anti-commutation relations effectively generate a Pauli-exclusion principle.

Due to the broken space reflection symmetry, the momentum distribution gets asymmetrically shifted from $k = 0$. We have shown that, while typically the momentum shifts smoothly with density, for $\theta = \pi$ there may be direct transitions between the SF₀ and SF_π phases.

Close to the pseudo-fermion limit $\theta \approx \pi$ a partially paired phase of a superfluid atomic and a paired component can be found to stable for large fillings $\rho \gtrsim 1.5$. A simple mean-field picture can be used for the illustration of this exotic quantum phase.

The mean-field analysis suggests that some of the features may be robust in more than one dimension. A possible generalization of the PP phase to a two-dimensional variant of the pseudo-AHM, even though an interpretation as an anyon-model would be inappropriate in this case, could be an interesting topic of further research.

Acknowledgments

We thank Guixin Tang, Min Gong and Luis Santos for their invaluable discussions. WZ and SG acknowledge hospitality of KITPC Beijing. WZ is supported by the NSFC under Grant No.11305113, Youth Foundation of Taiyuan University of Technology 1205-04020102. SG acknowledges support of QUEST-LFS and the DFG Research Training Group 1729. TCS is supported in China by the project GDW201400042 for the “high end foreign experts project”. YZ is supported by NSF of China under Grant Nos. 11234008 and 11474189, the National Basic Research Program of China (973 Program) under Grant No. 2011CB921601, Program for Changjiang Scholars and Innovative Research Team in University (PCSIRT)(No. IRT13076). Simulations were partially carried out on the cluster system at the Leibniz University of Hannover, Germany.

[1] F. Wilczek, Magnetic Flux, Angular Momentum, and Statistics, *Phys. Rev. Lett.* **48**, 1144 (1982).

[2] R. B. Laughlin, Anomalous Quantum Hall Effect: An Incompressible Quantum Fluid with Fractionally Charged Excitations, *Phys. Rev. Lett.* **50**, 1395 (1983).

[3] B. I. Halperin, Statistics of Quasiparticles and the Hierarchy of Fractional Quantized Hall States, *Phys. Rev. Lett.* **52**, 1583 (1984).

[4] F. D. M. Haldane, Fractional statistics in arbitrary dimensions: A generalization of the Pauli principle, *Phys. Rev. Lett.* **67**, 937 (1991).

[5] F. E. Camino, W. Zhou, and V. J. Goldman, Realization of a Laughlin quasiparticle interferometer: Observation of fractional statistics, *Phys. Rev. B* **72**, 075342 (2005).

[6] E.-A. Kim, M. Lawler, S. Vishveshwara, and E. Fradkin, Jordan-Wigner Transformation for Quantum-Spin Systems in Two Dimensions and Fractional Statistics, *Phys. Rev. Lett.* **95**, 176402 (2005).

[7] C. Nayak, S. H. Simon, A. Stern, M. Freedman, and S. Das Sarms, *Rev. Mod. Phys.* **80**, 1083 (2008).

[8] A. Yu. Kitaev, Fault-tolerant quantum computation by anyons, *Annals Phys.* **303** 2 (2003).

[9] Y. Shena, Q. Ai and G. L. Long, Detection of anyon's braiding and identification of anyon entangled states in optical microcavities, *Physica A* **410**, 88 (2014).

[10] G. R. Feng, G. L. Long, and R. Laflamme, Experimental simulation of anyonic fractional statistics with an NMR quantum-information processor, *Phys. Rev. A* **88**, 022305 (2013).

[11] J. W. Pan, S. Gasparoni, R. Ursin, G. Weihs, and A. Zellinger, Detection of anyons braiding and identification of anyon entangled states in optical microcavities, *Nature* **423**, 417 (2003).

[12] J. Zhang, C. Xie, K. Peng, and P. Loock, Anyon statistics with continuous variables, *Phys. Rev. A* **78**, 052121 (2008).

[13] B. Paredes, P. Fedichev, J. I. Cirac, and P. Zoller, Anyons in Small Atomic Bose-Einstein Condensates, *Phys. Rev. Lett.* **87**, 010402 (2001).

[14] L. M. Duan, E. Demler, and M. D. Lukin, Controlling Spin Exchange Interactions of Ultracold Atoms in Optical Lattices, *Phys. Rev. Lett.* **91**, 090402 (2003).

[15] A. Micheli, G. K. Brennen, and P. Zoller, A toolbox for lattice-spin models with polar molecules, *Nat. Phys.* **2**, 341 (2006).

[16] M. Aguado, G. K. Brennen, F. Verstraete, and J. I. Cirac, Creation, Manipulation, and Detection of Abelian and Non-Abelian Anyons in Optical Lattices, *Phys. Rev. Lett.* **101**, 260501 (2008).

[17] L. Jiang, G. K. Brennen, A. V. Gorshkov, K. Hammerer, M. Hafezi, E. Demler, M. D. Lukin, and P. Zoller, *Nat. Phys.* **4**, 482 (2008).

[18] T. Keilmann, S. Lanzmich, L. McCulloch, and M. Roncaglia, Statistically induced phase transitions and anyons in 1D optical lattices, *Nature Comm.* **2**, 361 (2011).

[19] S. Greschner, and L. Santos, The Anyon Hubbard Model in One-Dimensional Optical Lattices, *Phys. Rev. Lett.* **115**, 053002 (2015).

[20] C. Sträter, S. C. L. Srivastava and A. Eckardt, Floquet realization and signatures of one-dimensional anyons in an optical lattice, arXiv:1602.08384.

[21] L. Cardarelli, S. Greschner and L. Santos, Engineering interactions and anyon statistics by multicolor lattice-depth modulations, arXiv:1604.08829.

[22] S. Greschner, G. Sun, D. Poletti, L. Santos, Density-Dependent Synthetic Gauge Fields Using Periodically Modulated Interactions, *Phys. Rev. Lett.* **113**, 215303 (2014).

[23] Y. J. Hao, Y. B. Zhang, and S. Chen, Ground-state properties of one-dimensional anyon gases, *Phys. Rev. A* **78**, 023631 (2008).

[24] Y. J. Hao, Y. B. Zhang, and S. Chen, Ground-state properties of hard-core anyons in one-dimensional optical lattices, *Phys. Rev. A* **79**, 043633 (2009).

[25] A. del Campo, *Phys. Rev. A* **78**, 045602 (2008).

[26] Y. J. Hao, and S. Chen, Dynamical properties of hard-core anyons in one-dimensional optical lattices, *Phys. Rev. A* **86**, 043631 (2012).

[27] H. L. Guo, Y. J. Hao, and S. Chen, Quantum entanglement of particles on a ring with fractional statistics, *Phys. Rev. A* **80**, 052332 (2009).

[28] R. A. Santos, F. N. C. Paraan, and V. E. Korepin, Quantum phase transition in a multicomponent anyonic Lieb-Liniger model, *Phys. Rev. B* **86**, 045123, (2012).

[29] J. Arcila-Forero, R. Franco, J. Silva-Valencia, Critical points of the anyon-Hubbard model, arXiv:1604.02466

[30] G. X. Tang, S. Eggert, and A. Pelster, Ground-state properties of anyons in a one-dimensional lattice, *New J. Phys.* **17**, 123016 (2015).

[31] L. M. Wang, L. Wang, and Y. B. Zhang, Quantum walks of two interacting anyons in one-dimensional optical lattices, *Phys. Rev. A* **90** 063618 (2014).

[32] S. R. White, Density matrix formulation for quantum renormalization groups, *Phys. Rev. Lett.* **69**, 2863 (1992); Density-matrix algorithms for quantum renormalization groups, *Phys. Rev. B* **48**, 10345 (1993); U. Schollwöck, The density-matrix renormalization group, *Rev. Mod. Phys.* **77**, 259 (2005).

[33] A. Wagner, A. Nunnenkamp, C. Bruder, Mean-field analysis of spinor bosons in optical superlattices, *Phys. Rev. A* **86**, 023624 (2012).

[34] T. Mishra, S. Greschner, and S. Santos, Density-induced geometric frustration of ultra-cold bosons in optical lattices *New J. Phys.* **18**, 045016 (2015).

[35] A. K. Kolezhuk, F. Heidrich-Meisner, S. Greschner and T. Vekua, Frustrated spin chains in strong magnetic field: dilute two-component Bose gas regime, *Phys. Rev. B* **85**, 064420 (2012).

[36] A. J. Daley, J. M. Taylor, S. Diehl, M. Baranov, and P. Zoller, Atomic three-body loss as a dynamical three-body interaction, *Phys. Rev. Lett.* **102**, 040402 (2009).